Fracture-induced polymeric grating structures

C.C. Lin*, F. Yang**, J.W. Chin***, L. Sung*** and S. Lee*

*National Tsing Hua University, Hsinchu 30013, Taiwan, slee@mx.nthu.edu.tw
**University of Kentucky, Lexington, KY 40506, USA
***National Institute of Standards and Technology, Gaithersburg, MD 20899, USA

ABSTRACT

Fracture-induced structuring (FIS) is found in the polymer thin film sandwiched between two relatively rigid flat plates by simply separating apart the plates, which produces a complementary set of micro/nano scale nonsymmetrical periodic polymer ripple gratings on both plates. FIS is a potential candidate to be a low-cost and high-throughput nanopatterning technique, however, the the cracking mechanism of FIS is still not fully understood. In this study, FIS gratings were observed to follow the direction of the maximum in-plane shear stress induced by external separating-load. Furthermore, the result of gamma-irradiation effect shows that homogeneous/glassy and brittle material properties of polymer thin film is essential to cause uniform and smooth cracking. More phenomena such as primary/secondary gratings and competed rupture are also discussed in this paper. The results of this study can be applied to nanopatterning and nanotechnology.

Keywords: fracture-induced structuring, polymer thin film, mechanical instability, cracking, nanopatterning.

1 INTRODUCTION

Manipulating and utilizing the phenomenon of natural instability of polymeric materials has become a significant technique in nanopatterning and nanotechnology. Some instability phenomena can be used as tools to measure material properties at the nanoscale [1-4], and others can be used to replicate nano-pattern transferring [5-7] or control nano-pattern forming [8-11]. A mechanical instability of peeling approach by simply splitting a polymeric thin film sandwiched between two relatively rigid flat plates was developed to form sub-60-nm half-pitch gratings over large surface area, which is termed FIS; and it produced a complementary set of nonsymmetrical straight line grating patterns on two plates [12-14]. Nevertheless, its grating formation and cracking mechanism are still vague [14]. To the best of our knowledge, the FIS patterns reported in literatures are straight line gratings only, which limits its application [12-17]. In contrast to the peeling method, here we use uniaxial tension to produce submicron grating patterns and name our method as tensil-FIS. The mechanical mechanism for tensile-FIS follows the fracture-induced patterning. We investigate the cracking mechanism in the polymeric thin film by using geometrically simplified polymeric thin films.

2 EXPERIMENTAL

2.1 Tensile-FIS

Figure 1a-d shows the schematic of tensile-FIS processes. A mr-I8030 PMMA-based resist of nanoimprint (Micro Resist Technology GmbH) and glass slides of 25 mm x 25 mm x 1 mm (Paul Marienfeld GmbH&Co.) were used as the polymeric thin film and top/bottom plates, respectively. After spin-coating (Fig. 1a), hot pressing was performed on a Carver hot-press (model C). The temperature was held at 170°C for 5 min to ensure the adhesion (Fig. 1b). The sandwiched specimen was mounted with 3M double-sided tapes on a universal tensile machine (Hung Ta Instrument Co.) with a pair of flat-plate grips. Separation was processed at 25°C at a constant crosshead speed of 0.028±0.002 mm/s (Fig. 1c). After separation, ripple gratings were formed on the polymer thin films on both top and bottom plates (Fig. 1d).

While doing tensile-FIS with long-rectangular polymeric resist (Fig. 1e-h), a FH6400L PMMA-base photoresist (Fuji-Hunt) was used to conduct photolithography on a 4” silicon wafer using a mask aligner (Karl-Suss) (Fig. 1e). After the steps of photolithography to determine the sizes of the long-rectangular polymeric resists and flood exposure to make the polymeric resists non-photosensitive (Fig. 1f), the patterned 4” silicon wafer was cut into 25 mm x 25 mm chips. A same size un-patterned silicon chip was placed on the patterned chip to make the sandwiched specimen and carry out the tensile-FIS process (Fig. 1g-h). Several rounds of tensile-FIS were performed in order to confirm the repeatability. Topographic imaging and analysis was achieved using a Dimension 3100 AFM (Digital Instrument Inc.) with NSC 15/3 tapping-mode probes (μmasch). At least six different locations were measured and characterized on each sample.

2.2 Gamma-irradiation

Gamma-irradiation was performed on liquid-state mr-I8030 resist using Co-60 as a gamma-ray source with the dose rate of 30 kGy/h at Radiation Application Technology Center in the Institute of Nuclear Energy Research, Lungtang, Taiwan. The gamma-irradiation was carried out at 25°C in air. The irradiated liquid-state resist was used to carry out the tensile-FIS. At least two samples were analyzed by AFM per sampling interval.

NSTI-Nanotech 2011, www.nsti.org, ISBN 978-1-4398-7139-3 Vol. 2, 2011

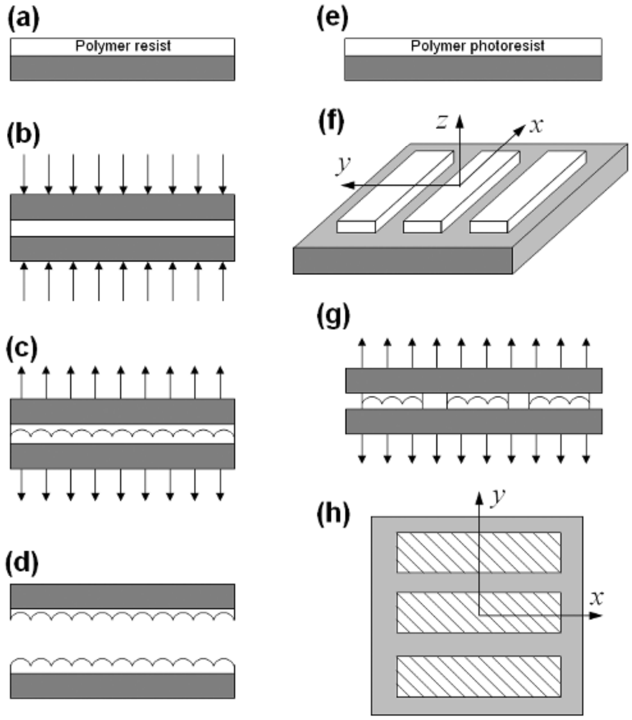

Figure 1: Schematics of tensile-FIS process.

2.3 Materials Properties Measurements

A DSC 200 F3 (Netzsch) was used to characterize the T_g change of mr-I8030 resist. Temperature was swept from 40 to 170 °C at a heating rate of 2 °C/min. The FTA125 contact angle goniometer (First Ten Ångstroms Inc.) with test liquids of DI water, ethylene glycol (99%, Mallinckrodt Baker Inc.) and diiodomethane (99%, Acros Organics Inc.) was used to measure the contact angle of mr-I8038 resist thin film with thickness of 300 nm on glass substrate.

The effect of gamma-irradiation on the elastic properties of mr-I8030 thin films was investigated by nanoindentation using Hysitron TriboScope^{TM} nanoindenter (Hysitron Inc.) with a Berkovich diamond tip. Two types of indentation tests were carried out at 25°C using load-control mode to eliminate the viscoelastic effect during the unloading segments [18-20]. The Young's modulus and Poisson's ratio of the Berkovich diamond tip are 1140 GPa and 0.07, respectively, and the Poisson's ratio of mr-I8030 thin film obtained from bulge test is 0.39 [21]. The present results were acquired using the loading/unloading time of 2 s and holding time of 20 s by analyzing the data at the contact depth of 50±5 nm.

3 RESULTS AND DISCUSSION

Figure 2a-d shows the AFM micrographs of the grating patterns formed by the tensile-FIS with large polymeric film (based on the process of Fig. 1a-d. The relation between spatial wavelength (λ) and polymer film thickness (h) is $\lambda = (3.12 \pm 0.46)h$, which is close to the proportional rule of the contact instability conducted by using glass substrate/contactor [8,9]. The size of grating domain can be as large as more than one centimeter square, while the orientation of gratings in each domain is random. If we use long-rectangular polymeric thin film to carry out tensile-FIS (using the process of Fig. 1e-h), a single domain of grating structure is observed and its orientation is about 45° with respect to the long edge of the long-rectangular polymeric resists (Fig. 2e-f). Such behavior is due to the asymmetric geometry, which confines the stress distribution in the long-rectangular polymeric film. For the long-rectangular polymeric film, the directions of the principal stresses (σ_x and σ_y) induced by the tensile loading in the z-direction are along the x- and y- axes, respectively (see Fig. 1f for the definition of coordinate). This results in the maximum in-plane shear stress in the direction of 45° with respect to the principal axes and the initiation of local yielding following the Tresca criteria during the separation processing. Note that local stress not only controls the deformation and cracking behavior, its variation also causes the deviation of grating orientation and/or change of spatial wavelength locally (Fig. 2e-f).

We investigated the effect of the gamma-irradiation on the properties of the polymeric films and the film cracking in tensile-FIS. Table 1 lists the material properties of the polymeric resists before and after exposing to the gamma-irradiation. The decrease in T_g is a result of the decrease in molecular weight, which represents a decline of stiffness and increase in viscosity [22]; and the increase in the breadth of transition evidences an increase in heterogeneity [23]. According to the results of nanoindentation, the Young's moduli are 4.53±0.28, 4.27±0.30 and 3.97±0.31 GPa, and hardness are 0.35±0.06, 0.31±0.07 and 0.28±0.06 GPa for the dose of 0, 100 and 200 kGy, respectively, which directly confirms the changes of elastic properties. The change of the contact angle in the non-polar test liquid (diiodomethane) indicates that only the change in molecular weight influences the surface energy (the contact angles of polar test liquids are unchanged so the results are not shown). According to previous studies, the spatial wavelength is independent of the adhesion strength and surface energy [12-13]. Figure 3a shows that the spatial wavelength (λ) of the tensile-FIS gratings increases slightly with the dose. This result is similar to the effect of separation temperature [12]. However, we found there are twill-like patterns on the 100 kGy-irradiated gratings and dislocation-like patterns on the 150 kGy-irradiated gratings (Fig 3b-d). Note that AFM micrograph for non-irradiated specimen is shown in Fig. 2(d). The gratings are eventually vanished when the dose is 200 kGy. This result implies that the heterogeneity and decline of the stiffness of the irradiated-polymeric thin film disturb the propagation of cracking [12]. The other evidence is that we often found competed rupture phenomenon in the non-irradiated polymeric thin films (Fig. 3e, 4b), while it hardly occurred in the highly irradiated polymeric thin films. Competed rupture is defined that, at the instant of fracturing, the convex and concave crack paths (relative to bottom plate) inside the polymeric thin film occur sequential randomly (inset of Fig. 3e), so that it results in the gratings with both convex and concave patterns in the same area (Fig. 3e). If the convex and concave cracks take place simultaneously and cracks connect to each other, delamination would be observed (Fig. 4b). Uniform and smooth crack propagation is supposed to be responsible for competed rupture phenomenon.

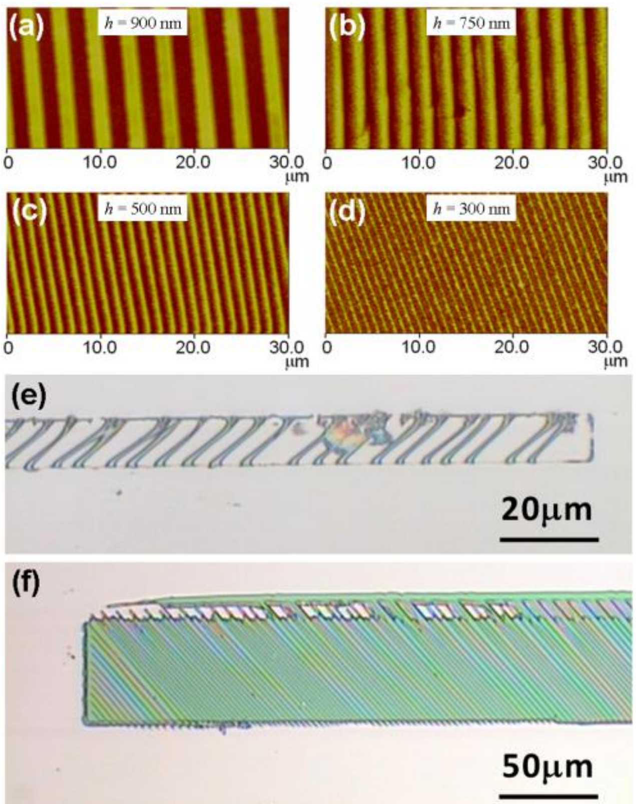

Figure 2: Images of the tensile-FIS grating patterns.

Dose [kGy]	T_g [°C]	Breadth of transition [°C]	Contact angle with diiodomethane
0	115±2	50±4	24.2°±1.0°
50	105±2	60±4	23.3°±0.8°
100	97±2	70±4	20.1°±0.5°
150	90±2	80±4	17.6°±0.5°
200	82±2	88±4	11.4°±0.5°

Table 1: Gamma-irradiation effect on the material properties of polymeric thin films.

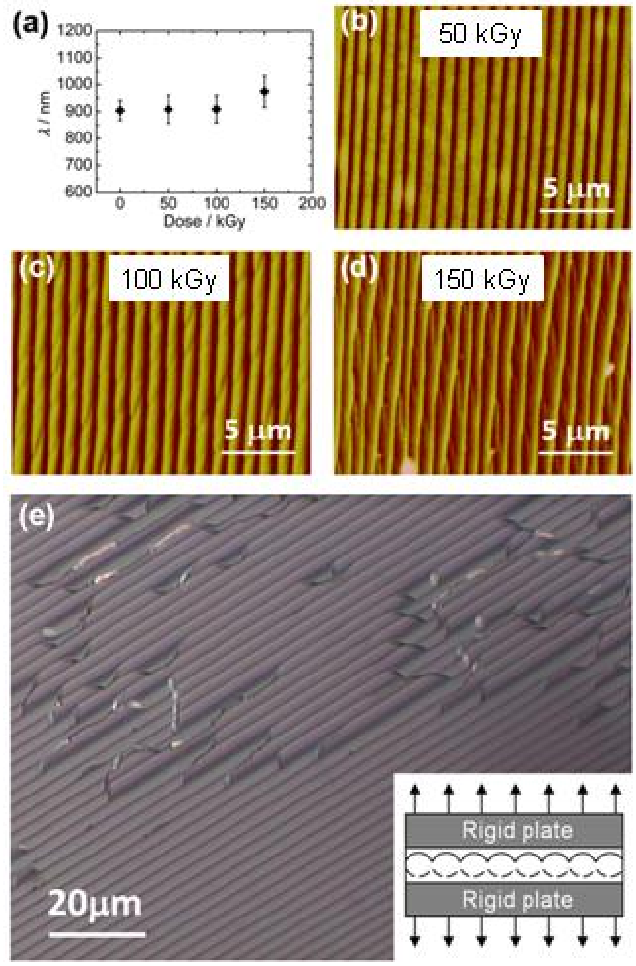

Figure 3: Results of gamma-irradiation effect and competed rupture phenomenon.

A tricky question is that cracking follows the primary direction of the maximum in-plane shear stress in the polymeric thin film, what happens with the other direction? Indeed they do follow both primary and secondary directions of maximum shear stresses that are mutually orthogonal to each other (Fig. 4a-c). Cracking in the secondary direction is unapparent and appears only occasionally. Similarly, orthogonal secondary gratings can also be seen in Ref. [17]. Note that the other difference between the primary and secondary gratings is the contrast of the amplitude (i.e. crack path selecting) of gratings. However, the conditions for the occurrence of orthogonal secondary gratings are still unknown.

In order to show how to control the structuring of FIS gratings, we conducted a single special separation by using two square glass plates that are almost the same in size. The sandwiched specimen with nearly defect-free polymeric thin film was separated by a point load applied manually at one corner of the top plate normal to film surface. Note that the bottom of the sandwiched specimen was fully attached on a fixed working-table. An amazing quarter of concentric circle FIS pattern was produced (Fig. 4d). This implied that

NSTI-Nanotech 2011, www.nsti.org, ISBN 978-1-4398-7139-3 Vol. 2, 2011

different FIS-pattern is possible to create if the proper design is applied.

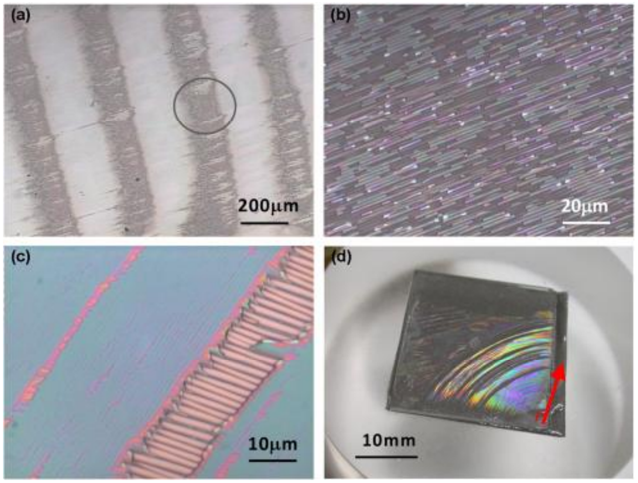

Figure 4: Orthogonal tensile-FIS patterns and a quarter of concentric circle FIS pattern. (b) shows the enlarged details in the circle area on (a).

4 CONCLUSIONS

In summary, we have proposed an experiment that shows the FIS gratings follow the direction of the maximum in-plane shear stress induced by external separating-load. Unlike the other mechanical instabilities that can cause island, ribbon or labyrinth patterns [2-11], FIS produces grating patterns only. Local stress state determines the grating orientation while the variation of local stress plays a key role to deviate orientation and/or change spatial wavelength locally. Homogeneous/glassy and brittle film material property is required to cause uniform and smooth cracking for FIS gratings. Compared with regular primary gratings, the mechanisms of competed rupture phenomenon and secondary gratings are more complicated.

REFERENCES

[1] J. Huang, M. Juszkiewicz, W. H. de Jeu, E. Cerda, T. Emrick, N. Menon and T. P. Russell, Science, 317, 650, 2007.

[2] N. Bowden, S. Brittain, A. G. Evans, J. W. Hutchinson and G. M. Whitesides, Nature, 393, 146, 1998.

[3] J. Genzer and J. Groenewold, Soft Matter, 2, 310, 2006.

[4] J. Y. Chung, A. J. Nolte and C. M. Stafford, Adv. Mater., 23, 349, 2011.

[5] E. Schäffer, T. Thurn-Albrecht, T. P. Russell and U. Steiner, Nature, 403, 874, 2000.

[6] E. Schäffer, S. Harkema, M. Roerdink, R. Blossey and U. Steiner, Adv. Mater., 15, 514, 2003.

[7] N. Wu and W. B. Russel, Nano Today, 4, 180, 2009.

[8] W. Mönch and S. Herminghaus, Europhys. Lett., 53, 525, 2001.

[9] V. Shenoy and A. Sharma, Phys. Rev. Lett., 86, 119, 2001.

[10] R. Mukherjee, R. C. Pangule, A. Sharma and I. Banerjee, J. Chem. Phys., 127, 064703, 2007.

[11] J. Y. Chung, A. J. Nolte and C. M. Stafford, Adv. Mater., 21, 1358, 2009.

[12] L. F. Pease III, P. Deshpande, Y. Wang, W. B. Russel and S. Y. Chou, Nat. Nanotechnol., 2, 545, 2007.

[13] C. C. Lin, F. Yang and S. Lee, Langmuir, 24, 13627, 2008.

[14] B. Freund, Nat. Nanotechnol., 2, 537, 2007.

[15] T. C. Lin, L. C. Huang, T. R. Chou and C. Y. Chao, Soft Matter, 5, 3672, 2009.

[16] Y. Cai and B. Z. Newby, J. Mater. Res., 25, 803, 2010.

[17] H. Zeng, B. Zhao, J. N. Israelachvili and M. Tirrell, Macromolecules, 43, 538, 2010.

[18] B. J. Briscoe, L. Fiori and E. Pelillo, J. Phys. D: Appl. Phys., 31, 2395, 1998.

[19] A. H. W. Ngan and B. Tang, J. Mater. Res., 17, 2604, 2002.

[20] C. K. Liu, S. Lee, L. P. Sung and T. Nguyen, J. Appl. Phys., 100, 033503, 2006.

[21] C. K. Huang, W. M. Lou, C. J. Tsai, T. C. Wu and H. Y. Lin, Thin Solid Films, 515, 7222, 2007.

[22] L. M. Clayton, T. G. Gerasimov, M. Cinke, M. Meyyappan, J. P. Harmon, Polym. Bull., 52, 259, 2004.

[23] S. R. Tatro, G. R. Baker, K. Bisht, J. P. Harmon, Polymer, 44, 167, 2003.